Lack of triangularity in SAR interferometric phases

Francesco De Zan, German Aerospace Center (DLR), Oberpfaffenhofen, Germany
email:francesco.dezan@dlr.de, tel. +49 (0) 8153 28 2150, fax +49 (0) 8153 28 1135
Mariantonietta Zonno, Politecnico di Bari, Italy
Paco López-Dekker, German Aerospace Center (DLR), Oberpfaffenhofen, Germany

Abstract

If three SAR images are available, it is possible to form three interferograms. In some cases the phases of the three averaged interferograms will not agree among each other and indicate a sort of phase excess or deficit (which we call "lack of triangularity"). In this paper we illustrate theoretically which models can explain such phenomenon and show some real-data examples. The observation of lack of triangularity might be useful to derive informations on the target and also as a warning that the scatterer presents a temporal covariance matrix which is not intrinsically real.

1 Introduction

This paper focuses on the concept of lack of triangularity in SAR interferometry. To observe this effect it is necessary to have three images able to interfere with each other from which three interferograms can be generated. If the interferograms are averaged spatially and the phases are combined in a circular way ($\phi_{12}+\phi_{23}+\phi_{31}$), the result might be different from zero. The lack of compensation could also simply point to the effects of statistical noise, but we are interested in this paper in non-trivial cases in which its systematic character reveals some physical cause.

2 Theory and examples

Calling i_n the $n^{\mathtt{th}}$ image in a coregistered stack, the interferogram between image n and image k will be

$$I_{nk} = |I_{nk}| \exp(j\phi_{nk}) = < i_n \, i_k^* > \tag{1}$$

where the asterisks stands for the complex-conjugate and the brakets denote some spatial averaging. It is possible then to define the phase [1]

$$\Phi_{nkh} = \phi_{nk} + \phi_{kh} + \phi_{hn} \tag{2}$$

Under many circumstances the three phases will compensate each other out so that the result will be zero (modulo 2π), up to some statistical noise. There are however cases in which this compensation will not happen and this lack of triangularity points to some deeper physical effect. These are the cases we are particularly interested in: the covariance matrix of the data is intrinsically complex, it cannot be made real by a simple phase calibration.
It has to be stressed that the operation of spatial averaging is necessary to reveal possible deviations from zero (*non-triangularities*); in fact, for single pixels, one can trivially show that it is always $\Phi_{nkh} \equiv 0$.

The concept of lack of triangularity presented here is analogous to the concept of excess geometric phase and three-point Bargmann invariant found in physics (e.g. [2]).

2.1 Phase terms that respect triangularity

It is useful to mention physical effects on the phase that will not break triangularity. In general, all delaying effects that can be attributed to each image are of this kind, like tropospheric delays. For example, if the phase of an small area is affected by a tropospheric delay of ϕ_n (one phase per image), the interferometric phase between two images will see the differential troposheric delay:

$$\phi_{nk} = \phi_n - \phi_k \tag{3}$$

and $\Phi_{nkh} = 0$ since all terms ϕ_n, ϕ_k, ϕ_h will appear twice in the sum (2) with opposite signs.
Similar reasoning can be conducted for phase effects caused by target motion (ground deformation) and topography in the presence of a normal baseline.
It is important to understand which effects do not break triangularity, since their presence is irrelevant. For instance, it is not necessary to worry about phase calibration (troposphere, topography, motion) if we are only interested in Φ_{nkh}.

2.2 Effects that can break triangularity

More interesting for the purpose of this paper are effects that can potentially break triangularity. The simplest example is volume scattering with normal baseline variations.

2.2.1 Volume scattering

As a first illustrative example we cite the coherence resulting from infinite volumes and an exponential attenuation of the signal derived in [3]:

$$\gamma_{nk} = \frac{1}{1 + jk_{nk}d} \tag{4}$$

where $k = 2\pi/h$ is the vertical differential wavenumber, d is the two-way penetration depth and h the height of ambiguity. With three images a possible set of k's is $k_{12} = k_{23} = -0.5k_{31}$ (two equal baselines), with $k_{12} + k_{23} + k_{31} = 0$. It is then immediate to verify that the complex quantity

$$\gamma_{12}\,\gamma_{23}\,\gamma_{31} = \frac{1}{1 + jk_{12}d}\;\frac{1}{1 + jk_{23}d}\;\frac{1}{1 + jk_{31}d} \tag{5}$$

does not have zero phase for any $d > 0$.

The coherences described by (4) are shown [3] to belong to a circle of diameter 1 and center (1/2,0) in the complex plane. If the phase was simply proportional to the baseline, there would be no volume but a single scattering layer at a defined height. This is indeed a way to see it: the phase Φ_{nkh} highlights a non-linearity in the phase dependence on the wavenumber (k).

In general it is possible to demonstrate interesting relations between the scattering profile $f(z)$ and the phase behavior. The interferogram is the Fourier transform of the profile and has the characteristics of an autocorrelation

$$R(k) = \int f(z)e^{jkz}dz \tag{6}$$

because the profile is real and positive (spectrum). Separating now the phase and amplitude components of the interferogram

$$R(k) = A(k)e^{j\phi(k)} \tag{7}$$

one can derive the following relations

$$\phi'(0) = \mathrm{E}[z] = \mu_z \tag{8}$$

$$A''(0) = -\,\mathrm{E}[(z - \mu_z)^2] \tag{9}$$

$$\phi'''(0) = -\,\mathrm{E}[(z - \mu_z)^3] \tag{10}$$

$$A^{IV}(0) = \mathrm{E}[(z - \mu_z)^4] \tag{11}$$

which tell us that the derivatives in zero are related to the central moments of the profile (spectrum). In $k = 0$ even derivatives of ϕ and odd derivatives of A are all equal to zero, because of the Hermitian symmetry of $R(k)$.

In particular, developing with Taylor approximation, for the tomographic case we have:

$$\Phi_{123} \approx -0.5\,\mathrm{E}[(z - \mu_z)^3]k_{12}\,k_{23}\,k_{31} \tag{12}$$

which shows how the phase excess is directly dependent on the profile skewness $\mathrm{E}[(z - \mu_z)^3]$ for small baselines. A real data illustration of triangularity break due to volume decorrelation is given in **Figure 1**. Three acquisitions of a TerraSAR-X crossing-orbit experiment are combined and the resulting phase differs from zero by several dozens of degrees. The two slaves are separated from the master by 1 and 5 days. The azimuth variations are mainly caused by a variation of the baselines within the scene, typical of the crossing orbit geometry. More details on the crossing-orbit experiment can be found in [4].

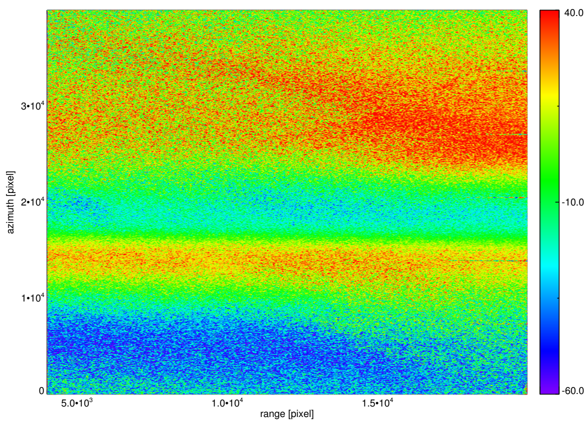

Figure 1: Lack of triangularity over Ronne's ice shelf (Antarctica) acquired by TerraSAR-X. The color scale is in degrees.

2.2.2 Propagation in variable dielectric

Another reason that could give rise to systematically imperfect compensation is a variation of soil moisture according to the model presented in [1]. There it is assumed that the scattering comes from targets at different depths, with propagation phases which depend both on the moisture state and the depth. The resulting effect could also be described as volumetric but the volume consists in just a few centimeters of soil and the moisture variation plays the role of normal baseline (changing the vertical wavenumber). There are indeed attempts to conduct tomographic reconstructions in small depths as in [5]. Although the mathematical expressions are different, the complex coherences modeled in [1] also belong almost perfectly to Dall's circle for infinite volumes mentioned above.

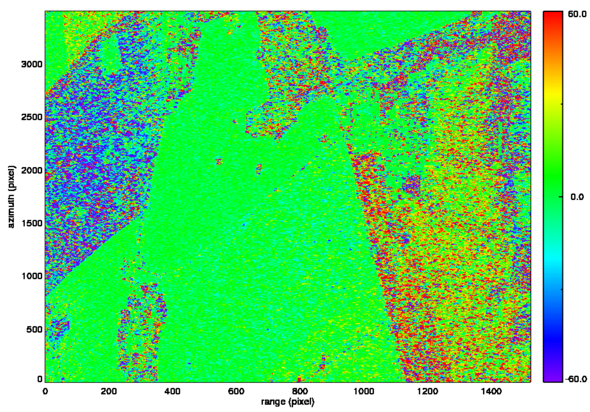

Figure 2: Lack of triangularity over agricultural fields (ESAR, L-band). The color scale is in degrees.

For the case of soil moisture variation we show in **Figure 2** the phase Φ_{nkh} for three images acquired over agricultural fields in three different days by DLR's ESAR sensor, operated in L-band. **Figure 3** shows the lack of triangularity in three L-band images acquired over Mt. Etna. For the area toward the montain summit, since there are no trees, the moisture variation hypothesis seems the most likely to explain the phase excess.

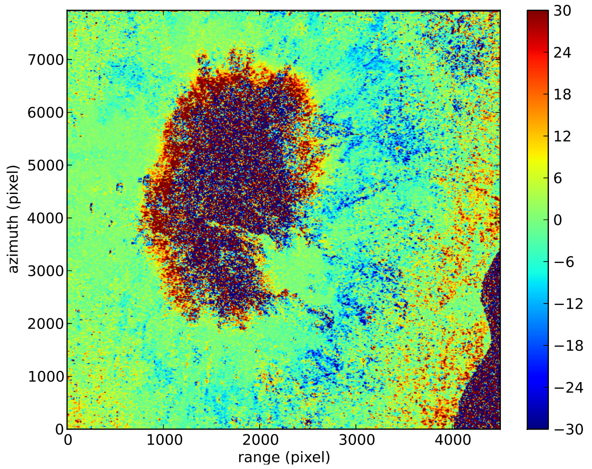

Figure 3: Lack of triangularity for Mt. Etna (Italy) acquired by PALSAR. The color scale is in degrees.

All the physical explanations proposed so far require that two (or more) different contributions are present in the averaging window and that they change phase independently from each other. For instance one could have in a certain image $y_1 = a + b$ and in a second $y_2 = a + be^{j\varphi}$, if only the second contribution changes its phase. The expected value of the interferogram is

$$\mathrm{E}[y_1 y_2^*] = \mathrm{E}[|a|^2] + \mathrm{E}[|b|^2]e^{-j\varphi} \tag{13}$$

with the usual assumption of uncorrelation of the scattering mechanisms ($\mathrm{E}[ab^*] = 0$). The resulting coherences will describe curves (in this case circles) in the complex plane as φ varies. This is a possible interpretation of the coherences measured by the TropiSCAT experiment (ESA, 2011-2012), which acquired almost continously radar data over the tropical forest from a tower in French Guiana. Many of the coherences computed during one day describe curves in the complex plane, like the one presented in **Figure 4**.

The physical variable driving the phase change could be the dielectric constant of sapwood, which is known to vary diurnally with water content and fluid chemistry [6] and directly affects the propagation of electromagnetic waves inside the trees.

The advantage of the TropiSCAT experiment is that it provides a calibrated phase, therefore coupling effects between coherence magnitude and phase are apparent. For normal repeat-pass satellite data this is not the case and the lack of triangularity reveals the same effects in a subtler way.

2.2.3 Statistical variation

The final example of lack of triangularity, not particularly interesting from the perspective of this paper, is the natural statistical variation of sample covariance matrices with respect to ideal covariances. This component is enough to break the perfect triangularity of an ideal real-valued coherency matrix. Indeed one can see the phase-linking algorithm [7, 8] as a tool to restore triangularity in the phases of an interferometric stack "corrupted" by statistical (speckle) noise.

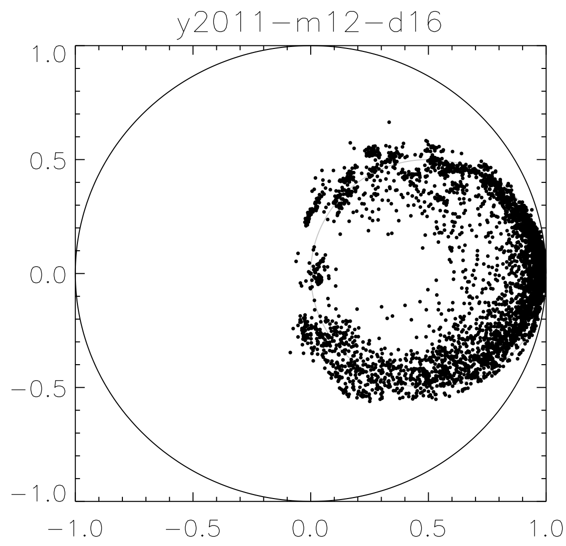

Figure 4: One example of the complex coherences for the HH channel of the TropiSCAT experiment (day 2011-12-16, 400-600MHz)

However for such algorithms it is crucial to distinguish natural statistical mismatches from geophysical signals, since they are typically based on the hypothesis that the temporal covariance matrix of the scatter is real, apart from propagation terms. The phase mismatch associated with statistical noise will be different for each averaging window and therefore no systematic bias is expected. This fact allows to distinguish interesting mismatches from trivial ones: if the excess phase is spacially correlated it can not be a statistical effect. The magnitude of the mismatch will also be an interesting indication, since it will not be reduced by multilooking as regular statistical noise.

3 Possible applications

The most interesting fact about the phase Φ_{mkh} is that it is immune to phase calibration. It is therefore possible to detect volume scattering with phases even without having to rely on a reference target or a PSI analysis to perform a phase calibration.

When the presence of volume scattering can be excluded (thanks to *a priori* information or because the normal baselines are small enough), a phase mismatch in three interferograms indicates that additional effects are at work. It could be moisture variations in soils like in [1] or in the trees as suggested in this paper.

The detection of any such effect is relevant e.g. if a phase linking algorithm [7, 8] is applied to filter the phases in a stack. This algorithm is applied early in stack processing, when calibration is not available. The presence of a Φ_{mkh} deviating from zero is at least a warning that the hypothesis of intrinsically-real covariance is not valid and results of phase linking might be seriously affected (model mismatch). At the moment, we do not have a correction for the phase linking algorithm that accomodates the lack of triangularity.

4 Conclusions

This paper has shown with theory and examples that interferometric phase mismatches between three SAR images are not unusual and can be linked to scattering effects. Their value stays in that they can be detected prior to phase calibration. More work is still needed to check the validity of the physical explanations which have been suggested, in particular to confirm the relation of interferometry with soil moisture and tree water status.

5 Acknowledgments

The authors thank ESA for the TropiSCAT campaign data. FDZ thanks F. Rocca for recognizing that the coherences in the moisture interferometric model [1] reside on the circle discuss in [3].

References

[1] De Zan, F.; Parizzi, A.; Prats-Iraola, P.; López-Dekker, P., *A SAR Interferometric Model for Soil Moisture*, IEEE Transactions on Geoscience and Remote Sensing, accepted for publication, 2013.

[2] Mukunda, N. and Simon R., *Quantum Kinematic Approach to the Geometric Phase,* Annals of Physics, vol. 228, no. 2, 1993.

[3] Jørgen Dall, *InSAR Elevation Bias Caused by Penetration Into Uniform Volumes*, IEEE Transactions on Geoscience and Remote Sensing, vol. 45, n. 7, 2007.

[4] Wollstadt, S.; López-Dekker, P.; Prats-Iraola, P.; De Zan, F.; Busche, T. and Krieger, G., *1 and 5 Day Differential INSAR Under Crossing Orbits with TerraSAR-X*, IGARSS, 2012.

[5] Keith Morrison, *Mapping Subsurface Archaeology with SAR*, Archaeol. Prospect., vol. 20, 2013.

[6] McDonald, K. C.; Zimmermann, R.; Kimball, J.S. *Diurnal and Spatial Variation of Xylem Dielectric Constant in Norway Spruce (Picea abies [L.] Karst.) as Related to Microclimate, Xylem Sap Flow, and Xylem Chemistry*, IEEE Transactions on Geoscience and Remote Sensing, vol. 40, n. 9, 2002.

[7] Monti Guarnieri, A. and Tebaldini, S., *On the exploitation of target statistics for SAR interferometry applications,* IEEE Trans. Geosci. Remote Sensing, vol. 46, no. 11, 2008.

[8] Ferretti, A.; Fumagalli, A.; Novali, F.; Prati, C.; Rocca, F.; Rucci, A., *A New Algorithm for Processing Interferometric Data-Stacks: SqueeSAR,* IEEE Trans. Geosci. Remote Sensing, vol.49, no.9, 2011.